Early haemodynamic changes observed in patients with epilepsy, in a visual experiment and in simulations

Rollings, David T.; Assecondi, Sara; Ostwald, Dirk; Porcaro, Camillo; Mccorry, Dougall; Bagary, Manny; Soryal, Imad; Bagshaw, Andrew P.

DOI:
10.1016/j.clinph.2015.07.008

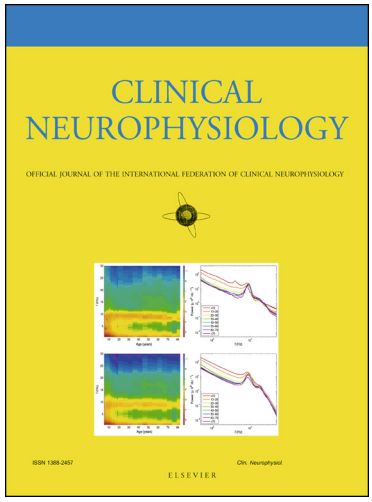

Early haemodynamic changes observed in patients with epilepsy, in a visual experiment and in simulations

David T. Rollings, Sara Assecondi, Dirk Ostwald, Camillo Porcaro, Dougall McCorry, Manny Bagary, Imad Soryal, Andrew P. Bagshaw

PII: S1388-2457(15)00714-2
DOI: http://dx.doi.org/10.1016/j.clinph.2015.07.008
Reference: CLINPH 2007553

To appear in: *Clinical Neurophysiology*

Accepted Date: 8 July 2015

Please cite this article as: Rollings, D.T., Assecondi, S., Ostwald, D., Porcaro, C., McCorry, D., Bagary, M., Soryal, I., Bagshaw, A.P., Early haemodynamic changes observed in patients with epilepsy, in a visual experiment and in simulations, *Clinical Neurophysiology* (2015), doi: http://dx.doi.org/10.1016/j.clinph.2015.07.008

Early haemodynamic changes observed in patients with epilepsy, in a visual experiment and in simulations

David T. Rollings[1,2,3*], Sara Assecondi [1,2], Dirk Ostwald[4], Camillo Porcaro[5], Dougall McCorry[3], Manny Bagary[6], Imad Soryal[3], Andrew P. Bagshaw[1,2]

[1]School of Psychology, University of Birmingham, Birmingham, UK

[2]Birmingham University Imaging Centre (BUIC), University of Birmingham, Birmingham, UK

[3]Department of Neuroscience, Queen Elizabeth Hospital Birmingham, Edgbaston, Birmingham, UK

[4]Max Planck Institute for Human Development, Berlin, Germany

[5]Laboratory of Electrophysiology for Translational Neuroscience (LET'S) – ISTC – CNR, Department of Neuroscience, Fatebenefratelli Hospital, Isola Tiberina, Rome, Italy

[6]Department of Neuropsychiatry, The Barberry, Birmingham, UK

* **Correspondence:**

David T. Rollings

Department of Neuroscience, Queen Elizabeth Hospital Birmingham, Egdbaston, Birmingham, B15 2WB, UK

Tel.: +44 1213716445

Fax: +44 1214149914

E-mail: David.Rollings@uhb.nhs.uk

Highlights

- Shifting event times leads to temporal bleeding of activation.
- Pre-spike analysis may improve concordance between the EEG and fMRI.
- Pre-spike analysis at 6 seconds preceding event minimises temporal overlap.

Keywords: epilepsy, haemodynamic response function, simulations, EEG-fMRI, visual stimulation, pre-spike response

Abstract

Objective. The objective of this study was to investigate whether previously reported early blood oxygen level dependent (BOLD) changes in epilepsy could occur as a result of the modelling techniques rather than physiological changes.

Methods. EEG-fMRI data were analysed from seven patients with focal epilepsy, six control subjects undergoing a visual experiment, in addition to simulations. In six separate analyses the event timing was shifted by either -9,-6,-3,+3,+6 or +9 seconds relative to the onset of the interictal epileptiform discharge (IED) or stimulus.

Results. The visual dataset and simulations demonstrated an overlap between modelled haemodynamic response function (HRF) at event onset and at +/-3s relative to onset, which diminished at +/-6s. Pre-spike analysis at -6s improved concordance with the assumed IED generating lobe relative to the standard HRF in 43% of patients.

Conclusion. The visual and simulated dataset findings indicate a form of "temporal bleeding", an overlap between the modelled HRF at time 0 and at +/-3s which attenuated at +/-6s. Pre-spike analysis at -6s may improve concordance.

Significance. This form of analysis should be performed at 6 seconds prior to onset of IED to minimise temporal bleeding effect. The results support the presence of relevant BOLD responses occurring prior to IEDs.

1. Introduction

Simultaneous acquisition of electroencephalography (EEG) and functional magnetic resonance imaging (fMRI) is a non-invasive technique (EEG-fMRI) that allows the indirect investigation of epileptiform neuronal activity in the human brain (for a review see Gotman et al., 2006). This method exploits the haemodynamic changes associated with interictal epileptiform discharges (IED) that are identified on the EEG. The concurrent blood oxygenation level dependent (BOLD) signal changes that accompany this activity are typically modelled with a haemodynamic response function (HRF) that peaks 5 – 6 seconds after the electrographic discharge (Glover, 1999, Friston et al., 1998). This canonical HRF, which for example may be derived from auditory responses in healthy volunteers (Glover, 1999), has previously been shown to be suitable for modelling BOLD changes related to IEDs (Bénar et al., 2002). However, studies have also demonstrated that the haemodynamic response in epilepsy is subject to variability in both peak timing and shape (Kang et al., 2003; Lemieux et al., 2008, Lu et al 2006), and that the sensitivity of EEG-fMRI to detect regions of activation can be improved by shifting the timing of the HRF relative to the IED (Bagshaw et al., 2004; Jacobs et al., 2007).

In a study by Hawco et al. (2007), they shifted the HRF to peak at 3 and 1 seconds prior to the onset of the IEDs, and successfully demonstrated BOLD responses with a similar degree of concordance to later peaking HRFs. These findings suggested the presence of metabolically-demanding neuronal activity, not visible on the EEG, but preceding the electrographically evident spike. The notion that haemodynamic responses might occur prior to electrographic epileptic activity was previously suggested by observations during the transition from the interictal to the ictal state by Federico et al. (2005), who observed BOLD changes several minutes prior to ictal onset. Makiranta et al. (2005) were also able to demonstrate BOLD changes preceding IEDs in an animal model following penicillin injection. They observed BOLD changes occurring several seconds prior to onset of the IED. For a review of other studies which have observed pre-ictal or pre-interictal haemodynamic changes, see Schwartz et al. (2011). It has been suggested that these early BOLD responses are

potentially more representative of the epileptogenic zone, resulting in improved localisation, since they may represent activity prior to propagation. For example, Jacobs et al. (2009) found that pre spike BOLD changes that occurred in nine of thirteen patients yielded more focal results than later responses with a strong degree of concordance with the electrographic spike field.

Given the clinical potential of EEG-fMRI recordings in patients with epilepsy, and the frequent difficulty in interpreting the results, any improvement in methodology and in the basic understanding of the technique would be welcome. However, the analysis strategy whereby HRFs are shifted to investigate haemodynamic activity prior to electrographic activity, while being relatively common in epilepsy studies, has not previously been applied to EEG-fMRI data from control subjects in task conditions. This leaves open the possibility that the observations made in patients with epilepsy regarding early peaking HRFs could be an artefact of the methodology. In order to address this issue, and to determine whether these observations are exclusive to spontaneously occurring, endogenous epileptiform events, we investigated early and late peaking HRFs in a control group participating in a visual task, as well as a group of patients with focal epilepsy. Since it is reasonable to assume that no such early BOLD changes would occur to random exogenous stimuli, their absence in an analysis with shifted HRFs would add validity to the pre-interictal BOLD responses that have been previously reported. We also used simulations to investigate how statistical values are altered by shifting HRFs and compared them to the patterns observed in patients with epilepsy and in task-related data.

2. Materials and Methods

2.1. Subjects

2.1.1. Visual experiment data

Six healthy volunteers (3 females, 3 males, mean age 21.8 years) were randomly selected from a group of fourteen subjects who had taken part in a previously reported experiment (Ostwald et al., 2010, Porcaro et al., 2010). All participants had normal or

corrected to normal visual acuity. Informed and written consent was obtained from the volunteers, and they were paid for their participation. The study was approved by the research ethics committee of the University of Birmingham.

The experiment, in brief, consisted of a sparsely presented 2Hz reversing checkerboard pattern in the left hemi-field (ISI 16.5–21s, discretised to 1.5s, spatial frequency 2 cycles per degree of visual angle, two contrast levels, high (CMichelson=1) and low (CMichelson=0.25)). Stimuli were presented with a central fixation cross for 1s (i.e. one checkerboard reversal), contrasts were randomized, and in total 85 trials of each contrast were presented. For full details see Ostwald et al., 2010; Porcaro et al., 2010.

2.1.2. Epilepsy patient data

Fifteen patients with a diagnosis of focal epilepsy were recruited from Consultant Neurologists with a special interest in Epilepsy, from the University Hospital Birmingham NHSF trust and The Barbary BSMH trust in accordance with National Health Service ethical approval (REC reference 06/Q2702/69). Patients were selected on the basis of frequency of IED (more than 10 IEDs per hour) and a seizure frequency of less than one per week. Written and informed consent was obtained, and the patients were screened to ensure suitability for scanning. Five subjects were excluded due to lack of IEDs during the scanning session, and three were excluded due to excessive movement in the scanner resulting in poor data quality. The seven patients included in the study had an age range of 18 – 40 years (mean 25.3 years, 5 females).

2.2. EEG-fMRI data acquisition

The same EEG acquisition protocol and equipment were used for the control subjects and the epilepsy patients. Continuous 64-channel EEG data were acquired at 5 kHz during scanning using MR-compatible EEG equipment (BrainAmp MR Plus, Brain Products, Munich, Germany). The EEG recording cap (Brain Products, Munich, Germany) consisted of 62 scalp electrodes distributed in accordance with the

international 10-20 system, with a further 2 electrodes to record ECG and ocular movements. Electrode impedances were kept below 10kΩ.

A 3T Philips Achieva MR Scanner (Philips, Netherlands) with an 8-channel SENSE head coil was used for the acquisition of echo-planar imaging (EPI) data, and a T1-weighted scan (1mm isotropic voxels) used for anatomical localisation of superimposed statistical parametric maps. For the visual experiment, EPI data were acquired from 20 slices covering occipital cortex in five runs of approximately 11 minutes (2.5x2.5x3mm voxels, TR 1500ms, TE 35ms, flip angle 80°, 441 volumes/run). For the data acquired from epilepsy patients, multiple scans of 6 minutes were acquired dependent on patient cooperation and comfort (patients 1 – 3 2.5mm isotropic voxels, TR 3000ms, TE 35ms, 50 slices, flip angle 85°, 120 volumes/run; patients 4 – 7, 3x3x4mm voxels, TR 2000ms, TE 35ms, 32 slices, flip angle 80°, 180 volumes/run).

2.3. EEG processing

Removal of MR gradient artefacts was performed offline using Brain Vision Analyser (Brain Products, Munich, Germany) using a template subtraction approach (Allen et al., 2000). Ballistocardiogram artefacts were removed using the Optimal Basis Set (OBS) plug-in (Niazy et al., 2005) to EEGLAB (Delorme and Makeig, 2004). For the epilepsy data, an experienced electroencephalographer marked the onset of any epileptiform electrographic discharges, categorising the events based on morphology, topography and duration. If a patient had more than one IED type, this was modelled within the same design matrix. Interictal events occurring within 15 seconds of each other were excluded from the analysis. No EEG processing was necessary for the visual dataset as only the stimulus event markers were needed.

Given the aim of this experiment was not to report solely on the localising potential of EEG-fMRI, but rather to ascertain the validity of the early BOLD changes, we defined concordance between EEG and fMRI based on localisation to the same brain lobe as identified from the surface EEG recording. If activation was seen in the

concordant lobe in the pre-event maps but absent in the standard HRF map then this was considered as an improvement in concordance.

2.4. fMRI processing

EPI data were processed in SPM5 (Wellcome Department of Imaging Neuroscience, UCL, UK). Initially the images underwent realignment for motion correction, followed by slice timing correction, anatomical normalisation to MNI space and then finally the data were smoothed with a Gaussian kernel (5mm for the visual data, 6mm for the epilepsy data). Images were flipped so that the right side of the image represents the right side of the brain (i.e. images are presented according to neurological convention).

The experimental data were modelled using a general linear model (GLM) in an event related design convolved with a canonical HRF implemented in SPM5 (Friston, 2007). The canonical HRF was modelled with time derivatives, and six motion correction parameters were also included in the analysis as multiple regressors. To change the peak of the HRF, the timing of the events in both the epilepsy and visual datasets were shifted by -3, -6 and -9 seconds for pre-event analysis and +3, +6 and +9 for post-event analysis. For both the visual and epilepsy datasets a threshold of $p<0.001$ uncorrected for multiple voxels was used but Bonferroni corrected to take account of the use of multiple HRFs.

2.5. ROI analysis

For each GLM analysis, performed on all data sets, a 5mm radius spherical region of interest (ROI) was defined around the activated voxel with the maximal t-statistic. The time course for each event was extracted over a 40/42 second time window, depending on the TR of the EPI acquisition, with 20/21 seconds pre and post event. These single event HRFs were then averaged for each analysis of a data set.

2.6. HRF Modelling

As an additional investigation into the effect of shifting event times on the statistical values identified from the GLM analysis, a series of model scenarios was investigated. We considered a task-like scenario, reproducing the visual data, and a random events scenario, reproducing the epilepsy data.

In both cases a single-voxel HRF was simulated according to the Balloon model (a generative model of the haemodynamic activity originating from a given stimulation scenario, based on differential equations as described in Buxton et al. (1998) and Friston et al. (2000)), with the following parameters: transit time = 0.98; O2 extraction rate = 0.736; time constant for signal decay = 1.54; stiffness = 0.33; neuroefficacy = 0.54; autoregulation = 2.46; V0 = 0.02. Each single-voxel time series was generated at 500 Hz and resampled at a range of TRs, to allow investigation of the effect of TR (1.5, 2.0, 2.5, and 3.0 seconds). White noise was added to obtain five SNR levels for each TR.

$$SNR = \frac{\sigma^2_{signal}}{\sigma^2_{noise}} = \{0.0, 0.2, 0.5, 0.7, 0.9\}$$

In the task-like scenario, we simulated the BOLD response to 85 stimuli, reproducing the parameters of the human visual stimulation (stimulus duration of 1 second, ISI 16.5–21s, discretised to 1.5s). In the random events scenario, we simulated the BOLD response to 38 random events with random timing mimicking epileptic spikes detected in patient 1, during the first run.

In both cases a basic GLM was fitted to the data, according to the following equation:

$$Y = \beta_0 X_0 + \beta_1 X_1 + \beta_2 X_2 + \varepsilon$$

Y is the simulated single-voxel time series, X_i is the i-th regressor (a constant term (X_0), the canonical HRF ($the\ Gamma\ function\ X_1$) and its time derivative (X_2) respectively) and ε is the random error term. The regressors were calculated by convolving the canonical HRF with the event times (task-related or random event), after shifting them from -10 TR to +10 TR in steps of TR/2 with respect to the

original times. We then fitted a GLM to the simulated data (with different TR and SNR) with shifted regressor and plotted the resulting T-statistic.

3. Results

3.1. Simulated Data

Figure 1 shows the results of the simulations, with the task-like scenario summarised in the upper panel, and the random (epilepsy-like) scenario in the lower panel. The results are shown for the four different TRs and for two of the five levels of noise (0 and 0.7). In general, the results are consistent with what was observed in the visual data set, with a similar pattern of reduction in T-value with shifting of event times (Figure 2). Across the range of TRs tested, the minimum T-values were observed when the event times were shifted by 5-7s either pre or post-event. For both task-like and random scenarios, the presence of noise reduced the prominence of the peak in T-value at time zero. As observed in the visual data (see below), there were secondary peaks in T-value for the task-like scenario, in keeping with the presence of prior and later events (i.e., with an ISI of 16.5–21s, shifting by 9s will result in overlap with the response to the preceding stimulus). Interestingly, when a longer TR was used the peak in T-values tended to shift to later times and the overall T-values reduced, presumably as a result of the sampling of the underlying HRF. Notably, the scenario that was most similar to the epilepsy data set (random events with considerable noise) demonstrated a pronounced effect of TR, with the improved characterisation of the HRF provided by shorter TRs leading to higher T-values and hence improved sensitivity. However, the reduction of T-values with preceding event times was slower (i.e., peak width was higher) with shorter TRs, leading to an increased likelihood of detecting a spurious pre-discharge activation. This broadening of the peak was also seen in the task-like scenario. Overall, particularly when a physiological level of noise was present, the simulations suggested that TR was not a major factor in determining whether it was likely that spurious activations would be present when shifting event times.

3.2. Visual Data

3.2.1. GLM results

In all subjects, as expected given the stimulation paradigm, maximal activation was seen in the right primary visual cortex using the canonical HRF. Significant activation was also seen in the same region across all pre- and post-stimulus HRFs at the relatively liberal threshold of $p<0.001$ that is often used in interictal epilepsy studies. The maximum T-statistics were associated with the standard peaking canonical HRF and the lowest with HRF-6 (Figure 2). Shifting the peak time of the HRF by 3 seconds either pre- or post-stimulus resulted in moderately robust activation, with the areas of maximal activation mostly confined to the visual cortex (Figure 3). As would be expected, when the peak of the HRF was shifted further from the stimulus event, less activation was noted and the T-statistic was reduced. The only exception was when the peak was shifted 9 seconds pre-stimulus, which resulted in a marginal increase in the average T-statistic and the number of activated clusters. This is likely to be a result of the timings of the stimulus presentation, as also confirmed by our simulations (see section 3.1 and Figure 1). This analysis suggests that a considerable amount of residual, artefactual activation is able to survive the statistical threshold often used in epilepsy studies (i.e., uncorrected $p<0.001$), but that this activity is minimised when shifting the event times by 6s.

3.2.2 ROI Analysis

As expected, the extracted time course showed a very consistent canonical response for each trial when modelled with the standard HRF, with the maximal signal change peaking at about 5 seconds post stimulus (Figure 3). A canonical response could also be seen at HRF-3 and HRF+3, although as expected the peak signal change fell at around 7 seconds and 4 seconds respectively, in line with the idea that these analyses were sampling the actual response to the stimuli presented at time zero. There was no convincing canonical shaped response seen in any of the other pre- or post-event analyses.

3.3. Epilepsy Data

3.3.1. Patients

The demographics and clinical details of the seven patients included in the study are summarised in Table 1. Patient 4 had two distinct IED types, although the right temporal sharp waves recorded from this patient failed to demonstrate any significant activation. The IEDs occurred randomly as isolated events in the EEG in all patients, with four IEDs excluded from analysis in patient 1 due to close proximity of the discharges.

3.3.2. GLM results: HRF

Using a threshold of $p<0.001$ uncorrected for multiple voxels but Bonferroni corrected to take account of the use of multiple HRFs (height threshold $t>3.6$), patients 1 and 6 did not show any significant activation associated with the standard peaking HRF (Table 2). Concordance with the electrographic spike field and the maximally activated region was seen in patient 4 (left temporal sharp waves and activation evident in left hippocampus and left medial temporal gyrus) with the standard peaking HRF. Concordant activation was also seen in patient 5 (left frontal sharp waves with activation in left middle frontal gyrus) and patient 7 (left temporal spikes with activation in the left middle temporal gyrus); however these were not the clusters with the greatest T statistic. With the standard HRF, areas of deactivation were noted in 6 of the 7 patients but they were not concordant with the spike field in any of the patients.

3.3.3. GLM Results: Early HRF

In line with the results from the simulations and the visual data set, we concentrated our analysis to events shifted by 6s prior to the real IEDs (i.e., HRF-6). For patient 1 at HRF-6, there was an increase in BOLD signal in the inferior aspect of the superior temporal gyrus and the right rolandic operculum, showing a degree of concordance with the spike field (right temporal sharp waves). Right and left inferior temporal activation was seen in patient 2 when the right temporal IEDs were modelled with HRF-6. In patient 3 no prespike activation survived statistical threshold. Patient 4

demonstrated an increase in BOLD signal in the right inferior temporal gyrus into the supramarginal gyrus at HRF-6; this was contralateral to the electrographic IEDs. Data from patient 5 yielded similar results between the three pre-spike analyses, with more robust activation seen in the left inferior frontal region with HRF-6, concomitant with the spike field of left frontal sharp waves. No activation was noted when using HRF or HRF-3 models for patient 6, however at HRF-6, activation was noted in the electrographically concordant lobe, although this was not the maximally activated cluster.

A small area of deactivation in the left hippocampus, concordant with the spike field, was evident in patient 3 at HRF-6. The only other dataset to demonstrate deactivation near the region of the spike field was patient 5 with changes in the left rectal/midorbital gyrus at HRF-3,-6,-9 with additional deactivation seen in the left hippocampus at HRF-9.

From this group of patients, concordance was evident in 4/7 (57%) when shifting the HRF to peak 6 seconds earlier, including patients 1, 2 and 6 where no concordant activation was evident in the standard HRF analysis.

3.3.4. GLM Results: Late HRF

Post event analyses for all patients demonstrated significant activation at HRF+6, however only patient 5 demonstrated activation concordant with the electrographic spike field. This activation was observed in the most rostral area of the left superior frontal gyrus at HRF+6, with this activation moving more left lateral at HRF+9. Deactivations were observed in five patients at HRF+6, with left inferior frontal and middle orbital deactivation seen in patient 5 at HRF+6, which was concordant with the electrographic spike field of this patient.

3.3.5. ROI Analysis

There was considerable variability in the haemodynamic responses to individual IEDs for each patient, and this was common across all HRF analyses (figure 4). This

variability resulted in a mean time course which did not show a clear canonical shaped response in the majority of the data, with only a few exceptions. In the original HRF analysis the mean time course from patient 3 was the only one to show maximum signal change at around 5-6 seconds, an observation which was not evident in the other patients. The prespike analysis for patient 2 demonstrated a clear maximum signal change at 3 seconds and 6 seconds for HRF-6 and HRF-9 respectively, and had a resemblance of a canonical shape. This was not the case in any of the other prespike analysis. The mean time course for patient 2 (figure 4) showed peak signal change at 3 seconds when modelled with HRF -6 and peaked at 6 seconds when modelled with HRF-9.

4. Discussion

The primary aim of this study was to ascertain if the event related GLM design used in most EEG-fMRI studies of patients with epilepsy is appropriate in modelling pre-spike BOLD changes. To this end we applied the same pre- and post-spike analysis to a control group who participated in a visual experimental paradigm, and performed a series of simulations of the relevant experimental scenarios. We observed pre and post-spike activation in the visual dataset despite the exogenous stimuli where one would not expect any pre event signal changes. The most notable changes occurred at HRF-3 and HRF+3, where significant activation was noted in the visual cortex in all datasets. The area of activation was similar to that activated when modelled with the standard canonical HRF. We explain these findings in terms of a simple overlap of the HRFs used to model these responses. The HRF shifted by +/-3s overlaps with the increase signal in the fMRI time course associated with the event, resulting in a pattern of activation similar to the HRF at time 0, as in essence the same event is being modelled. This effect could be termed “temporal bleeding” as the rise and fall in the fMRI time course “bleed” into HRFs modelled at -3s and +3s respectively. The results from the time series extraction from our visual dataset highlight signal changes in the time series that overlap with the modelled canonical HRF.

Further corroboration for this interpretation came from the simulations, which also demonstrated that simply by the mechanics of the analysis considerable T values can

be achieved when shifting event times. Both the visual and simulated data showed a gradual rather than an abrupt drop in T-value from event onset, thus allowing some overlap in pre and post event analyses. From the time series, it is evident that shifting the HRF by 3 seconds either way causes an associated shift in the maximum signal change corresponding to the direction of shift, either pre or post event. When shifting the HRF to peak 3 seconds prior to the event our results show that some of the activation/deactivations may overlap with the HRF modelled with actual event times and thus would not reliably reflect genuine pre/post spike changes. These observations are what would be expected from the simulations. Random event simulations with 70 per cent noise, a simulation of a physiological scenario, demonstrated only slight variations in timing when using different TRs, indicating differing TRs do not substantially alter the results. Based on these findings, when using this method of analysis, shifting event timings by seconds, rather than number of TRs, would be a valid approach.

In our study, pre-spike analysis at HRF-6 demonstrated activation in 5 of the 7 (71%) epilepsy patients, with activation occurring in the spike field in 4 of the 7 (57%) datasets. However not all the concordant clusters contained the maximum T value. In our findings, 3 (43%) of the 7 patients showed activation clusters concordant with the spike field in addition to containing the maximally activated voxel in prespike analysis. In a study by Jacobs et al. (2009), prespike BOLD responses were observed in 11 of the 13 (85%) studies, comparable to our study. They demonstrated focal activations concordant with the spike field in 4 studies, with the HRF peaking -9 to -5 seconds, and in 7 of the studies when the HRF peak was -3 to +1 seconds; this increased concordance observed closer to the actual event time may reflect the overlap in the models as previously discussed. One of the first studies to investigate early BOLD changes was conducted by Hawco et al. (2007), who demonstrated BOLD signal changes prior to scalp discharge. The degree of concordance between these early activations and the spike field was comparable to our study and that of Jacobs et al. (2009), with 5 of the 7 patients showing concordance in those that had early HRFs. From our study, one patient (#2) demonstrated clear signal changes in the time course peaking at 6 seconds when modelled with HRF-9 and at 3 seconds when modelled at HRF-6 without a clear change in signal with the standard HRF. From the

observations made in the visual dataset shifting the event time forwards caused the peak signal change in the time course to be shifted backwards, i.e. from 6 seconds to 3 seconds. This would indicate that the response from patient 2 at HRF-9 would be the genuine BOLD response and the signal changes seen at HRF-6 would result from this temporal bleeding effect. Given these findings it is possible that the BOLD signal changes observed 9 seconds prior to the IEDs could represent genuine pre spike activation. While electrophysiologically this is a considerable amount of time, it is consistent with previous work and suggestive of metabolically-demanding processes occurring considerably before a scalp discharge.

A clear distinction between the time courses observed for the visual and epilepsy datasets is the absence of consistent responses on an event-by-event basis from the epilepsy data. Figure 3 shows obvious and robust responses to brief visual stimuli, whereas the responses to IEDs are much more variable. Non-canonical HRFs have been commented upon previously (Lu et al., 2006; Lemieux et al., 2008), and our data also highlights that not all IEDs, despite being morphologically similar in the EEG, are associated with BOLD signal increases consistent with a canonical HRF. This variability in the BOLD signal between individual IEDs within the same subject may explain why EEG-fMRI studies in focal epilepsy are often plagued by low statistical values. It is not clear why IEDs of the same type within a subject vary in their BOLD response so much, but this may suggest variability in metabolic demand or in the mechanisms of generation.

The activity driving the early BOLD response does not appear to result in an identifiable electrographic discharge (Jacobs et al., 2009), but given the substantial area of synchronized cortex required to generate an electrographic discharge visible on scalp EEG (Ray et al., 2007; Tao et al., 2007), this is hardly surprising. This prespike activity has been shown to be more focal than later modelled responses (Jacobs et al., 2009) and thus prespike activations could potentially be more representative of the epileptogenic zone. The mechanism that drives these early BOLD changes has been the subject of considerable debate since they were first observed. In order to investigate the mechanisms underlying this phenomenon, Pittau et al. (2011) conducted an EEG-fMRI study comparing early observed BOLD

activations to intracerebral EEG recordings. In their study of 4 patients they found electrical discharges in the prespike period which corresponded to the early BOLD response in only one patient. They concluded that these commonly observed BOLD responses that precede epileptiform discharges are due to metabolic events starting prior to scalp spikes resulting from both neuronal and non-neuronal mechanisms. These findings demonstrating little electrical activity preceding scalp spikes aid in the explanation of the absence of prespike EEG power changes noted by Jacobs et al. (2009). Overall, these early BOLD responses are evidently a consistent phenomenon that is reproducible across studies in a variety of epilepsy subtypes in both adults and children (Schwartz et al 2011). Despite these observations it is not currently possible to reliably predict which IED or epilepsy type will demonstrate early BOLD changes. In our study of heterogeneous patients, no reliable and consistent pattern was evident.

Deactivations in epilepsy have been reported for both generalised and focal seizure disorders (Aghakhani et al., 2004; Bagshaw et al., 2004; Kobayashi et al., 2006; Stefanovic et al., 2005; Hamandi et al., 2006; Hawco et al, 2007; Moeller et al., 2008; Jacobs et al., 2009; Rathakrishnan et al., 2010). We observed pre-spike and post-spike deactivations, with deactivations notably less common than activations. Deactivations concordant with the spike field were evident in only two patients across all analyses (patients 3 and 5). Deactivations observed using the standard canonical HRF were often distant from the electrographic spike field and inconsistent given the heterogeneity of the group. A study by Rathakrishnan et al. (2010) noted a partial overlap between areas of deactivation with preceding activation. This observation was not evident in our findings apart from one patient (#5) who demonstrated deactivation concordant with both spike field and pre-spike activations at +3, +6 and +9 seconds post-spike. Our findings are also less consistent than those found by Jacobs et al. (2009) who found concordant deactivation precipitated by pre-spike activation in three of their subjects. Our observations could be due to the heterogeneity of our patient group and consequently suggest that IED type plays a pivotal role in the patterns of deactivation observed, both pre- and post-spike.

5. Conclusion

In summary, reliability of pre-spike changes observed in IEDs is highly variable and likely varies between subjects and IED types, and thus any improved concordance observed from this type of analysis should be viewed with caution. From the visual and simulated data we suggest that any pre/post-event analyses needs to be restricted to approximately 6 seconds either side of event onset. Although unlikely to eliminate the effects completely, this will serve to minimise the likelihood of temporal bleeding between models. This will be dependent to a degree on the TR used with a shorter TR slightly more likely to pick up spurious activations as compared to a longer TR. This relatively small influence of TR would suggest that restricting analyses to 6 seconds rather than a specified number of TRs (i.e., four to five TRs if TR=1.5s, two TRs if TR=3s) would be sufficient. More extensive studies with more homogenous groups of patients showing single IED types may yield more information about the factors which contribute to the observation and reliability of pre-spike fMRI

Conflict of Interest

None of the authors have any conflict of interest to disclose. We confirm that we have read the Journal's position on issues involved in ethical publication and affirm that this report is consistent with those guidelines.

Acknowledgements

This work was supported in part by grant number EP/F023057/1 from the UK Engineering and Physical Sciences Research Council (EPSRC).

References

Aghakhani Y., Bagshaw A. P., Bénar C. G., Hawco C., Andermann F., Dubeau F., Gotman J. fMRI activation during spike and wave discharges in idiopathic generalized epilepsy. Brain. 2004;127:1127-44.

Allen P.J., Josephs O., Turner R. A method for removing imaging artifact from continuous EEG recorded during functional MRI. Neuroimage. 2000;12:230-9.

Bagshaw A. P., Aghakhani Y., Bénar C. G., Kobayashi E., Hawco C., Dubeau F., Pike G. B., Gotman J. EEG-fMRI of focal epileptic spikes: analysis with multiple haemodynamic functions and comparison with gadolinium-enhanced MR angiograms. Hum Brain Mapp. 2004;22:179-92.

Bénar C. G., Gross D. W., Wang Y., Petre V., Pike B., Dubeau F., Gotman J. The BOLD response to interictal epileptiform discharges. Neuroimage 2002;17:1182-92.

Buxton, R. B., Wong, E. C., Frank, L. R. Dynamics of blood flow and oxygenation changes during brain activation: the balloon model. Magn Reson Med 1998;39:855-864.

Delorme A., Makeig S. EEGLAB: an open source toolbox for analysis of single-trial EEG dynamics including independent component analysis. J Neurosci Methods 2004;134:9-21.

Federico P., Abbott D. F., Briellmann R. S., Harvey A. S., Jackson G. D. Functional MRI of the pre-ictal state. Brain 2005;128:1811-7.

Friston K. J., Ashburner J., Kiebel S. J., Nichols T. E., and Penny W.D. Statistical Parametric Mapping: The Analysis of Functional Brain Images. Academic Press; 2007.

Friston K. J., Fletcher P., Josephs O., Holmes A., Rugg M. D., Turner R. Event-related fMRI: characterizing differential responses. Neuroimage 1998;7:30-40.

Friston, K. J., Mechelli, A., Turner, R., Price, C. J. Nonlinear responses in fMRI: the balloon model, Volterra kernels, and other hemodynamics. NeuroImage 2000;12:466-477.

Glover G. H. Deconvolution of impulse response in event-related BOLD fMRI. Neuroimage 1999;9:416-29.

Gotman J., Kobayashi E., Bagshaw A. P., Bénar C. G., Dubeau F. Combining EEG and fMRI: a multimodal tool for epilepsy research. J Magn Reson Imaging 2006;23:906-20.

Hamandi K., Salek-Haddadi A., Laufs H., Liston A., Friston K., Fish D. R., Duncan J. S., Lemieux L. EEG-fMRI of idiopathic and secondarily generalized epilepsies. Neuroimage 2006;31:1700-10.

Hawco C. S., Bagshaw A. P., Lu Y., Dubeau F., Gotman J. BOLD changes occur prior to epileptic spikes seen on scalp EEG. Neuroimage 2007;35:1450-8.

Jacobs J., Kobayashi E., Boor R., Muhle H., Stephan W., Hawco C., Dubeau F., Jansen O., Stephani U., Gotman J., Siniatchkin M. Hemodynamic responses to interictal epileptiform discharges in children with symptomatic epilepsy. Epilepsia 2007;48:2068-78.

Jacobs J., Levan P., Moeller F., Boor R., Stephani U., Gotman J., Siniatchkin M. Hemodynamic changes preceding the interictal EEG spike in patients with focal epilepsy investigated using simultaneous EEG-fMRI. Neuroimage 2009;45:1220-31.

Kang J. K., Bénar C., Al-Asmi A., Khani Y. A., Pike G. B., Dubeau F., Gotman J. Using patient-specific hemodynamic response functions in combined EEG-fMRI studies in epilepsy. Neuroimage 2003;20:1162-70.

Kobayashi E., Bagshaw A. P., Grova C., Dubeau F., Gotman J. Negative BOLD responses to epileptic spikes. Hum Brain Mapp 2006:27;488-97.

Lemieux L., Laufs H., Carmichael D., Paul J. S., Walker M. C., Duncan J. S. Noncanonical spike-related BOLD responses in focal epilepsy. Hum Brain Mapp 2008;29:329-45.

Lu Y., Bagshaw AP., Grova C., Kobayashi E., Dubeau F., Gotman J. Using voxel-specific hemodynamic response function in EEG-fMRI data analysis. Neuroimage. 2006;32:238-47.

Mäkiranta M., Ruohonen J., Suominen K., Niinimäki J., Sonkajärvi E., Kiviniemi V., Seppänen T., Alahuhta S., Jäntti V., Tervonen O. BOLD signal increase preceeds EEG spike activity-a dynamic penicillin induced focal epilepsy in deep anesthesia. Neuroimage 2005;27;715-24.

Moeller F., Siebner H. R., Wolff S., Muhle H., Boor R., Granert O., Jansen O., Stephani U., Siniatchkin M. Changes in activity of striato-thalamo-cortical network precede generalized spike wave discharges. Neuroimage 2008;39:1839-49.

Niazy R. K., Beckmann C. F., Iannetti G. D., Brady J. M., Smith S. M. Removal of FMRI environment artifacts from EEG data using optimal basis sets. Neuroimage 2005;28:720-37.

Ostwald D., Porcaro C., Bagshaw A. P. An information theoretic approach to EEG-fMRI integration of visually evoked responses. Neuroimage 210;49:498-516.

Pittau F., Levan P., Moeller F., Gholipour T., Haegelen C., Zelmann R., Dubeau F., Gotman J. Changes preceding interictal epileptic EEG abnormalities: comparison between EEG/fMRI and intracerebral EEG. Epilepsia 2011;52:1120-9.

Porcaro C., Ostwald D., Bagshaw A. P. Functional source separation improves the quality of single trial visual evoked potentials recorded during concurrent EEG-fMRI. Neuroimage 2010;50:112-23.

Rathakrishnan R., Moeller F., Levan P., Dubeau F., Gotman J. BOLD signal changes preceding negative responses in EEG-fMRI in patients with focal epilepsy. Epilepsia 2010;51:1837-45.

Ray A., Tao J. X., Hawes-Ebersole S. M., Ebersole J. S. Localizing value of scalp EEG spikes: a simultaneous scalp and intracranial study. Clin Neurophysiol. 2006;118;69-79.

Schwartz T. H., Hong S. B., Bagshaw A. P., Chauvel P., Bénar C. G. Preictal changes in cerebral haemodynamics: review of findings and insights from intracerebral EEG. Epilepsy Res 2011;97:252-66.

Stefanovic B., Warnking J. M., Kobayashi E., Bagshaw A. P., Hawco C., Dubeau F., Gotman J., Pike G. B. Hemodynamic and metabolic responses to activation, deactivation and epileptic discharges. Neuroimage 2005;28:205-15.

Tao J.X., Baldwin M., Hawes-Ebersole S., Ebersole J. S. Cortical substrates of scalp EEG epileptiform discharges. J Clin Neurophysiol 2007;24:96-100.

Figure Legends

Figure 1. Simulations. T-statistic obtained in the two scenarios considered (task-like and random events). Each line represents, for a specific TR, the t-statistic of the GLM fitting, as a function of the delay used when shifting the events. The scenario without added noise is depicted on the left while the scenario with 70% noise is depicted on the right. In every case the t-statistic peaks around zero and decreases when the event onset used to model the regressors is shifted in time. The periodicity seen in the task-like scenario, due to the periodicity of the stimuli, disappears when random event are considered, as in the random-events scenario.

Figure 2. Maximum t statistic across all HRF analysis for the 6 visual datasets. Greatest dip in T value occurs 6 seconds pre/post stimulus.

Figure 3. Visual dataset. Example from participant 5. Statistical t map (t>3.6, corrected for analysis with multiple HRFs) for HRF and HRF-3,+3 superimposed over subject specific T1 anatomical scan normalised to MNI space. Axial slice through HRF focused on maximally activated voxel. No clusters of activation were observed in the visual cortex at HRF-6,-9,+6,+9 with activated clusters here being random and distant. Extracted time course from ROI shows a plot for each event and mean (black line).

Figure 4. Epilepsy dataset. Example from two patients showing maximally activated clusters (t>3.6 Bonferroni corrected threshold) for standard HRF and pre event maps; HRF-6,-9. Bi inferior temporal activation seen in the pre event maps of patient 2 at HRF-6 and HRF-9 to sharp waves in the right temporal region. Left frontal sharp waves of patient 5 demonstrated clear activation evident in the left inferior frontal gyrus at HRF-6 and HRF -9. Extracted time course from ROI shows a plot for each event and mean (black line). Note, right side of MRI image represents the right side of the brain (neurological convention).

Patient	Age/Sex	Epilepsy/Seizure type	EEG	MRI	IED (#)
1	40/M	TLE/CPS	R T SW	R Oligoastrocytoma	137
2	30/M	TLE/CPS	R T SW	Normal	14
3	25/F	PLE/SPS,CPS & GTCS	R P Sp	Normal	15
4	18/F	TLE/CPS	L T SW	Normal	56
5	25/F	FLE/CPS	L F SW	Normal	59
6	21/F	TLE/CPS	L T Sp	Previous excision of L T Oligoastrocytoma	45
7	18/F	TLE/CPS	L T SW	L T DNET	17

Table 1. Summary of patients. Abbreviations: FE = focal epilepsy, TLE = temporal lobe epilepsy, FLE = frontal lobe epilepsy, PLE = parietal lobe epilepsy, SPS = simple partial seizures, CPS = complex partial seizures, GTCS = generalised tonic clonic seizures, R = right, L = left, F = frontal, T = temporal, P = parietal, SW = sharp wave, Sp = spike.

Patient	HRF	HRF-3	HRF-6	HRF-9	HRF+3	HRF+6	HRF+9
1	n/a	**R Sup Med Gyrus (3.86),** L Hippocampus, L Sup Med Gyrus	**R Inf T gyrus (3.87)**, R rolandic operculum	**L caudate (4.08)**, L fusiform gyrus.	**L caudate (4.16)**	**L Fusiform gyrus (3.97)**, R Fusiform Gyrus	**R Inf T Gyrus (4.20)**, R Sup T Gyrus, L Fusiform Gyrus,
2	**R Inf F Gyrus (4.00)**, R Sup F Gyrus.	**R Rectal Gyrus (3.69)**	**R Hippocampus (4.64),** L Fusiform Gyrus.	**L Fusiform Gyrus (6.03),** R Parahippocampal Gyrus.	**R Mid F Gyrus (4.52)**, R Rolandic Operculum	**R Mid F Gyrus (5.16)**, R Insula, R Precentral Gyrus	**R Insula (4.64)**, R Inf F Gyrus, R Putamen
3	**R Fusiform Gyrus (4.85)**	n/a	n/a	n/a	**R Hippocampus (6.21)**	**L Lingual Gyrus (3.83)**	**L Inf T Gyrus (6.09)**, R Cingulate, R Inf F Gyrus.
4	**L Hippocampus (4.44),** L Med T, L Mid F Gyrus	**R Sup F Gyrus (4.31),** L Parahippocampal Gyrus, L Amygdala	**R Inf T Gyrus (4.17)**, R Sup P	**R Inf P (4.47),** R Inf T Gyrus, L Mid F Gyrus	**R Fusiform Gyrus (3.77)**	**L Insula (3.75)**	**R Sup F Gyrus (3.97)**, L T Pole, L Sup Orbital Gyrus.
5	**L Hippocampus (3.63)**, L T Pole, L Mid F Gyrus	**L Mid F Gyrus (4.02)**	**L Inf F Gyrus (4.46),** L Sup F Gyrus, L Rectal Gyrus.	**L Mid Orbital Gyrus (4.41)**, L Inf F Gyrus, R Sup Orbital Gyrus	**L Mid Orbital Gyrus (4.22),** L Mid F Gyrus, L Sup Orbital Gyrus	**L Mid F Gyrus (4.61),** L Inf F Gyrus	**L Sup F Gyrus (4.11)**, L Inf F Gyrus
6	n/a	n/a	**R Thalamus (3.99),** L Fusiform Gyrus	**R Paracentral (3.70)**	n/a	**L Mid T Gyrus (3.82)**	**R Thalamus (4.39)**, L Med T Pole
7	**L Inf F Gyrus (4.08)**, L Mid T Gyrus, L Mid F Gyrus	**L Caudate (3.94)**	n/a	**Genu of Corpus Callosum (3.65)**	**L Sup Med Gyrus (3.93)**, R Mid F gyrus, L Mid F Gyrus	**R Sup Med Gyrus (4.90)**, L Mid F Gyrus	**L Inf O Gyrus (4.26)**, L Inf F Gyrus, L Mid T Gyrus

Table 2. Anatomical locations of activations across all HRF analyses. Regions highlighted in bold represent cluster with maximum t statistic for each analysis and the t value in parentheses.

Abbreviations: "n/a" = no activation survived threshold, R = right, L = left, F = frontal, T = temporal, P = parietal, O = occipital, Inf = inferior, Sup = superior, Med = medial, Mid = middle